Available online at www.sciencedirect.com
ScienceDirect
Journal of Sound and Vibration 300 (2007) 241–249
JOURNAL OF SOUND AND VIBRATION
www.elsevier.com/locate/jsvi

Dynamic characteristics of piezoelectric cylindrical transducers with radial polarization

Jin O. Kim*, Jung Gu Lee

Department of Mechanical Engineering, Soongsil University, 1 Sangdo-dong, Donjak-gu, Seoul 156-743, Republic of Korea

Received 21 February 2005; received in revised form 27 July 2006; accepted 3 August 2006
Available online 10 October 2006

Abstract

This paper presents the radial vibration characteristics of piezoelectric cylindrical transducers. Taking into account the piezoelectric anisotropy, dynamic differential equations of piezoelectric radial motion have been derived in terms of radial displacement and electric potential. Applying mechanical and electric boundary conditions has yielded a characteristic equation for radial vibration of the radially polarized piezoelectric cylinder. Theoretical calculations of the fundamental natural frequency have been compared with numerical and experimental results for transducers of several sizes, and have shown a good agreement.

1. Introduction

Many electromechanical sensors or actuators [1] used nowadays in various fields are based on piezoelectric phenomenon [2], which converts electric signals into mechanical vibrations and vice versa. Most piezoelectric transducers of a disc type use longitudinal vibrations in the thickness direction and a few uses torsional vibrations with shear motion in the circumferential direction as a torsional transducer [3].

On the other hand, piezoelectric cylindrical transducers have been introduced in several forms. A transducer polarized in the axial direction undergoes axial motion under the electric drive in the radial thickness direction, and is used as an aligner or a translator, for example in a scanning tunneling microscope [1]. A transducer polarized in the circumferential direction undergoes radial vibrations resulting from circumferential expansion and compression [4]. A transducer polarized in the radial direction undergoes radial vibrations, and is used for flow control [5] or for flow measurement [6].

This paper deals with the radial vibration of piezoelectric cylindrical transducers polarized in the radial direction. The behaviors of these transducers have been studied in some different point of view. The static behavior was derived for cylindrical ceramic tubes [7,8]. Dynamic characteristics of piezoelectric shells were derived by neglecting the shell thickness [9] or by assuming constant stress and displacement distribution along the thickness direction [10]. With regard for the anisotropy of piezoelectric materials of ceramic rings or cylinders, dynamic solutions for the radial displacement and electric potential were obtained in terms of

*Corresponding author. Tel.: +82 2 820 0662; fax: +82 2 820 0668.
E-mail address: jokim@ssu.ac.kr (J.O. Kim).

0022-460X/$ - see front matter
doi:10.1016/j.jsv.2006.08.021

Lommel functions as well as Bessel functions [11,12]. By reducing the anisotropic elastic properties to isotropic ones in terms of Young's modulus and shear modulus and maintaining the anisotropic dielectric and piezoelectric properties, the fundamental natural frequency of cylindrical transducers was conveniently calculated according to the sizes of the cylinder [13].

The purpose of this paper is to establish a formula for calculating the fundamental natural frequency of piezoelectric cylindrical transducers with consideration of the piezoelectric anisotropy but without relying on the inconvenient Lommel function. First of all, the differential equations of piezoelectric radial motion were derived in terms of radial displacement and electric potential. The characteristic equation of radial vibration was obtained by applying mechanical and electric boundary conditions. Theoretical calculations of the fundamental natural frequency are compared with numerical calculations and experimental observations for transducers of several sizes. The calculated results are also compared with the earlier results [13] of theoretical analysis simplifying the piezoelectric anisotropy into isotropy.

2. Theoretical analysis

The radial vibration characteristics of a piezoelectric cylindrical transducer are theoretically analyzed with consideration for the anisotropy of piezoelectric materials.

2.1. Problem formulation

A piezoelectric cylindrical transducer is schematically shown in Fig. 1. The piezoelectric cylinder has uniform electrodes on the inner surface of radius R_i and on the outer surface of radius R_o. Radial vibrations in the cylinder can be described in terms of the axisymmetric radial displacement $u(r, t)$ and electric potential $\phi(r, t)$, which are both functions of the radial coordinate r and time t.

The radial and circumferential components of normal stresses σ_r and σ_θ and the radial component of electric displacement D_r, incorporating piezoelectric effect, in the piezoelectric cylinder are expressed as follows [12].

$$\sigma_\theta = c_{11}^E \frac{u}{r} + c_{13}^E \frac{\partial u}{\partial r} + e_{31} \frac{\partial \phi}{\partial r}, \tag{1}$$

$$\sigma_r = c_{31}^E \frac{u}{r} + c_{33}^E \frac{\partial u}{\partial r} + e_{33} \frac{\partial \phi}{\partial r}, \tag{2}$$

$$D_r = e_{31} \frac{u}{r} + e_{33} \frac{\partial u}{\partial r} - \varepsilon_{33}^S \frac{\partial \phi}{\partial r}. \tag{3}$$

Here, e_{31}, e_{32}, e_{33} and ε_{33}^S are constants expressed as follows.

$$e_{3j} = c_{ij}^E d_{3i} \quad (i,j = 1,2,3), \tag{4a}$$

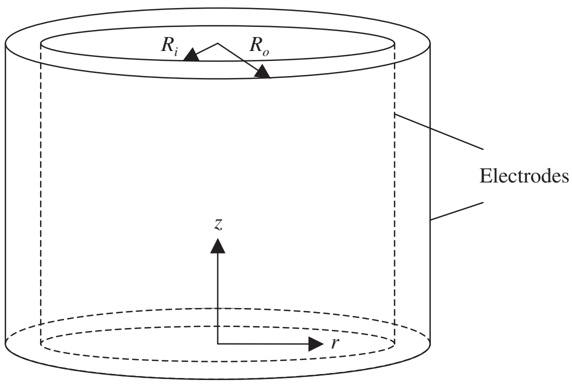

Fig. 1. Schematic diagram of a cylindrical transducer.

$$\varepsilon_{33}^S = \varepsilon_{33}^T - e_{3i}d_{3i}, \tag{4b}$$

where c_{ij}^E are the stiffness constants, d_{kl} are the piezoelectric strain constants, and ε_{33}^T is the dielectric permittivity. The stiffness constants can be related to compliance constants or technical constants [14].

The equation of motion derived from the force equilibrium is the following [15].

$$\frac{\partial \sigma_r}{\partial r} + \frac{\sigma_r - \sigma_\theta}{r} = \rho \frac{\partial^2 u}{\partial t^2} \tag{5}$$

and the electrostatic charge equation is the following [16].

$$\frac{1}{r}\frac{\partial}{\partial r}(rD_r) = \frac{\partial D_r}{\partial r} + \frac{D_r}{r} = 0, \tag{6}$$

where ρ is the mass density. Inserting Eqs. (1)–(3) into Eqs. (5) and (6) yields the following equations.

$$c_{33}^E\left(\frac{\partial^2 u}{\partial r^2} + \frac{1}{r}\frac{\partial u}{\partial r}\right) - c_{11}^E\frac{u}{r^2} + e_{33}\left(\frac{\partial^2 \phi}{\partial r^2} + \frac{1}{r}\frac{\partial \phi}{\partial r}\right) - e_{31}\frac{1}{r}\frac{\partial \phi}{\partial r} = \rho\frac{\partial^2 u}{\partial t^2}, \tag{7}$$

$$\varepsilon_{33}^S\left(\frac{\partial^2 \phi}{\partial r^2} + \frac{1}{r}\frac{\partial \phi}{\partial r}\right) = e_{33}\left(\frac{\partial^2 u}{\partial r^2} + \frac{1}{r}\frac{\partial u}{\partial r}\right) + e_{31}\frac{1}{r}\frac{\partial u}{\partial r}. \tag{8}$$

Eqs. (7) and (8) form a set of differential equations, that do not yield a solution. By eliminating the terms including $(e_{31}/r)\,\partial/\partial r$, Eqs. (7) and (8) turn out to be the following ones at the sacrifice of the accuracy in the solution.

$$\frac{\partial^2 u}{\partial r^2} + \frac{1}{r}\frac{\partial u}{\partial r} - \frac{c_{11}^E}{c_{33}^D}\frac{u}{r^2} = \frac{1}{c_L^2}\frac{\partial^2 u}{\partial t^2}, \tag{9}$$

$$\left(\frac{\partial^2 \phi}{\partial r^2} + \frac{1}{r}\frac{\partial \phi}{\partial r}\right) = \frac{e_{33}}{\varepsilon_{33}^S}\left(\frac{\partial^2 u}{\partial r^2} + \frac{1}{r}\frac{\partial u}{\partial r}\right), \tag{10}$$

where $c_L\,(=[c_{33}^D/\rho]^{1/2})$ in Eq. (9) is the propagation velocity of the longitudinal wave, and $c_{33}^D = c_{33}^E + {e_{33}}^2/\varepsilon_{33}^S$.

When the voltage applied to the electrodes is a harmonic function of time t with frequency ω, the displacement u and the electric potential ϕ are regarded as harmonic functions of time with the same frequency. Therefore, $u(r, t)$ and $\phi(r, t)$ can be expressed through the separation of variables in the following:

$$u(r,t) = \tilde{u}(r)\mathrm{e}^{\mathrm{i}\omega t}, \tag{11a}$$

$$\phi(r,t) = \tilde{\phi}(r)\mathrm{e}^{\mathrm{i}\omega t}. \tag{11b}$$

Substituting Eqs. (11a) and (11b) into Eqs. (9) and (10) provides the following governing equations:

$$r^2\frac{\mathrm{d}^2\tilde{u}}{\mathrm{d}r^2} + r\frac{\mathrm{d}\tilde{u}}{\mathrm{d}r} + (k^2r^2 - p^2)\tilde{u} = 0, \tag{12}$$

$$\frac{\mathrm{d}}{\mathrm{d}r}\left(r\frac{\mathrm{d}\tilde{\phi}}{\mathrm{d}r}\right) = \frac{e_{33}}{\varepsilon_{33}^S}\frac{\mathrm{d}}{\mathrm{d}r}\left(r\frac{\mathrm{d}\tilde{u}}{\mathrm{d}r}\right), \tag{13}$$

where $k\ (=\omega/c_L)$ is the wavenumber, and p is a constant defined as $p^2 = c_{11}^E/c_{33}^D$.

The solution of Eq. (12) has the following form:

$$\tilde{u}(r) = A_1J_p(kr) + A_2J_{-p}(kr). \tag{14}$$

After inserting Eq. (14) into Eq. (13), the solution of $\tilde{\phi}(r)$ is obtained as follows:

$$\tilde{\phi}(r) = \frac{e_{33}}{\varepsilon_{33}^S}\left[A_1J_p(kr) + A_2J_{-p}(kr)\right] + A_3\ \ln r + A_4. \tag{15}$$

The unknown constants A_1, A_2, A_3, and A_4 are determined according to the boundary conditions.

2.2. Characteristic equation

As shown in Fig. 1, the piezoelectric cylinder has an inner radius of R_i and an outer radius R_o. The transducer is driven by an electric voltage $V_0\ \mathrm{e}^{\mathrm{i}\omega t}$ applied between its inner and outer surfaces. Boundary conditions are established as follows:

$$\tilde{\sigma}_r = 0 \quad \text{and} \quad \tilde{\phi} = 0 \quad \text{at} \quad r = R_i, \tag{16a,b}$$

$$\tilde{\sigma}_r = 0 \quad \text{and} \quad \tilde{\phi} = V_o \quad \text{at} \quad r = R_o. \tag{16c,d}$$

Since the radial stress σ_r ($= \tilde{\sigma}(r)\mathrm{e}^{\mathrm{i}\omega t}$) has the formula as stated in Eq. (2), applying boundary conditions (16a–d) to Eqs. (14) and (15) yields the following equations.

$$f_1(k, R_i)A_1 + f_2(k, R_i)A_2 + \frac{e_{33}}{R_i}A_3 = 0, \tag{17a}$$

$$g_1(k, R_i)A_1 + g_2(k, R_i)A_2 + A_3 \ln R_i + A_4 = 0, \tag{17b}$$

$$f_1(k, R_o)A_1 + f_2(k, R_o)A_2 + \frac{e_{33}}{R_o}A_3 = 0, \tag{17c}$$

$$g_1(k, R_o)A_1 + g_2(k, R_o)A_2 + A_3 \ln R_o + A_4 = V_0, \tag{17d}$$

where

$$f_1(k, r) = c_{33}^D \frac{\mathrm{d}}{\mathrm{d}r}[J_p(kr)] + c_{31}^E \frac{J_p(kr)}{r}, \tag{18a}$$

$$f_2(k, r) = c_{33}^D \frac{\mathrm{d}}{\mathrm{d}r}[J_{-p}(kr)] + c_{31}^E \frac{J_{-p}(kr)}{r}, \tag{18b}$$

$$g_1(k, r) = \frac{e_{33}}{\varepsilon_{33}^S} J_p(kr), \tag{18c}$$

$$g_2(k, r) = \frac{e_{33}}{\varepsilon_{33}^S} J_{-p}(kr). \tag{18d}$$

Eliminating the constants A_3 and A_4 in Eqs. (17a–d) results in a set of two equations in a matrix form as follows.

$$\begin{bmatrix} B_{11} & B_{12} \\ B_{21} & B_{22} \end{bmatrix} \begin{bmatrix} A_1 \\ A_2 \end{bmatrix} = \begin{bmatrix} 0 \\ V_0 \end{bmatrix}. \tag{19}$$

$$\begin{aligned}
B_{11} &= R_o f_1(k, R_o) - R_i f_1(k, R_i) \\
B_{12} &= R_o f_2(k, R_o) - R_i f_2(k, R_i) \\
B_{21} &= g_1(k, R_o) - g_1(k, R_i) - \frac{R_o}{e_{33}} f_1(k, R_o) \ln \frac{R_o}{R_i} \\
B_{22} &= g_2(k, R_o) - g_2(k, R_i) - \frac{R_o}{e_{33}} f_2(k, R_o) \ln \frac{R_o}{R_i}
\end{aligned}$$

The unknown constants are determined by obtaining constants A_1 and A_2 from Eq. (19) and inserting them into Eqs. (17a) and (17b).

$$A_1 = -\frac{V_0}{\Delta}\left[R_o f_2(k, R_o) - R_i f_2(k, R_i)\right], \tag{20a}$$

$$A_2 = \frac{V_0}{\Delta}\left[R_o f_1(k, R_o) - R_i f_1(k, R_i)\right], \tag{20b}$$

$$A_3 = \frac{V_0}{\Delta}\frac{1}{e_{33}}\left[f_1(k,R_i)f_2(k,R_o) - f_1(k,R_o)f_2(k,R_i)\right], \tag{20c}$$

$$\begin{aligned} A_4 = \frac{V_0}{\Delta}\Big\{&\left[R_o f_2(k,R_o) - R_i f_2(k,R_i)\right]g_1(k,R_i) \\ &- \left[R_o f_1(k,R_o) - R_i f_1(k,R_i)\right]g_2(k,R_i) \\ &- \frac{R_i R_o \ln R_i}{e_{33}}\left[f_1(k,R_i)f_2(k,R_o) - f_1(k,R_o)f_2(k,R_i)\right]\Big\}, \end{aligned} \tag{20d}$$

where Δ represents the determinant of the matrix in Eq. (19).

Resonance occurs when the determinant Δ is equal to 0.

$$\Delta \equiv \begin{vmatrix} B_{11} & B_{12} \\ B_{21} & B_{22} \end{vmatrix} = 0. \tag{21}$$

Eq. (21) is the characteristic equation representing the resonance of a piezoelectric cylindrical transducer driven in the radial direction. Meanwhile, the mode shapes of the radial vibration can be obtained by inserting Eqs. (20a–b) into Eq. (14) and assuming a value of 1 for V_0/Δ for a relative displacement distribution.

2.3. Fundamental natural frequency

The results of the analysis described in the previous section can be verified by calculating the natural frequencies and comparing them with experimental observations. The unknown variable k in Eq. (21) can be calculated easily by using a root-finder function (FindRoot) available in Mathematica [17]. A successful search necessitates a good initial guess, which can be selected by the elastic natural frequency of a corresponding non-piezoelectric, i.e. elastic, cylinder. Once the wavenumber k is evaluated, the natural frequency f is obtained from the following relation:

$$f = \frac{kc_L}{2\pi}. \tag{22}$$

The piezoelectric material selected for the numerical calculation and experiment was PZT (EC-64), manufactured by EDO Co. The material properties are as summarized in Table 1, and they are similar to the values reported in other literature [18]. The properties converted in terms of the expressions in this paper are as in Table 2. Three transducers A, B, and C of different sizes were used in the research. Their outer radius R_o and inner radius R_i are seen in Table 3. The lengths of the transducers A, B, and C shown in Fig. 2 were 20, 15, and 12 mm, respectively, but these values were unnecessary in the calculations.

The piezoelectric natural frequencies of the fundamental mode for these transducers were calculated from Eq. (21) and listed in Table 3. The frequencies of the isotropic analysis [13] were also listed in Table 3 and compared with anisotropic analysis results. It appears that the discrepancy between two analysis results is larger for the cylindrical transducers with a smaller radius.

Table 1
Material properties of a PZT (EDO EC-64)

	Properties	Values
Mechanical	Mass density, ρ	$7500\,\mathrm{kg/m^3}$
	Elastic compliance, s_{11}^E, s_{22}^E	$12.8\times10^{-12}\,\mathrm{m^2/N}$
	s_{12}^E, s_{13}^E	$-4.2\times10^{-12}\,\mathrm{m^2/N}$
	s_{33}^E	$15.0\times10^{-12}\,\mathrm{m^2/N}$
Dielectric	Relative permittivity, $\varepsilon_{33}^T/\varepsilon_0$	1300
Electromechanical	Piezoelectric constant, d_{31}, d_{32}	$-127\times10^{-12}\,\mathrm{C/N}$
	d_{33}	$295\times10^{-12}\,\mathrm{C/N}$

Table 2
Converted properties of a PZT (EDO EC-64)

	Properties	Values
Mechanical	Elastic stiffness, c_{11}^E, c_{22}^E	$10.9 \times 10^9\,\mathrm{N/m^2}$
	c_{12}^E	$5.1 \times 10^9\,\mathrm{N/m^2}$
	c_{13}^E	$4.5 \times 10^9\,\mathrm{N/m^2}$
	c_{33}^E	$9.2 \times 10^9\,\mathrm{N/m^2}$
Dielectric	Permittivity, ε_{33}^T	$11.8 \times 10^{-9}\,\mathrm{C^2/Nm^2}$
Electromechanical	Piezoelectric constant, e_{33}	$15.7\,\mathrm{C/m^2}$
	e_{31}, e_{32}	$-7.1\,\mathrm{C/m^2}$

Table 3
Comparison of the natural frequencies of the fundamental mode calculated by anisotropic and isotropic analyses and by FEM and measured by an experiment for transducers of three sizes

Transducer	Size (mm)		Fundamental frequency (kHz)			
	Outer radius R_o	Inner radius R_i	Theoretical analysis		FEM	Measurement
			Anisotropic	Isotropic		
A	14.3	12.0	41.5	37.9	37.6	38.8
B	10.05	7.80	61.4	56.0	55.3	56.3
C	7.10	5.50	87.0	79.4	77.9	80.8

(A) (B) (C)

Fig. 2. Photograph of three transducers, whose sizes are listed in Table 3.

3. Comparison with numerical and experimental results

The theoretical results obtained in the previous section are compared with numerical and experimental results.

3.1. Numerical analysis by the finite-element method

In the previous section, the radial vibration characteristics of piezoelectric cylindrical transducers were theoretically analyzed. The analysis considered the anisotropy of piezoelectric materials and calculated the piezoelectric natural frequency of the fundamental mode. During the derivations the terms including $(e_{31}/r)\partial/\partial r$ in Eqs. (7) and (8) were eliminated to obtain solvable Eqs. (9) and (10). In order to confirm the validity of the analysis results, this section provides numerical results obtained by the finite element method.

A commercial finite-element software ANSYS was used to calculate the vibration modes and their natural frequencies of piezoelectric cylindrical transducers. Transducers A, B, and C were modeled by using SOLID5 element, which is a coupled-field element including piezoelectricity. The models were divided by 10 in the radial direction, by 40 in the circumferential direction, and 7, 6, and 5, in the axial direction for transducers A, B, and C, respectively.

With the electric boundary conditions on the inner and outer surfaces of the cylinder, modal analysis provided piezoelectric natural frequencies and mode shapes. As an example the fundamental mode of transducer A is shown in Fig. 3. Solid lines in the figure represent the deformed shape and show the cylinder expanded radially. The numerically calculated piezoelectric natural frequencies of the fundamental mode were listed in Table 3 and compared with the theoretically calculated results.

3.2. Experiments

Experimentally obtained piezoelectric natural frequencies for the piezoelectric cylindrical transducers shown in Fig. 2 were reported earlier [13], and they are cited in this section to compare with the calculated values. The resonance frequency of a transducer was measured using the Impedance Gain/Phase Analyzer (HP 4194A). The measured impedance curves displayed as a function of the frequency were shown in Fig. 4. The locations of local minimum impedance in the curves of Fig. 4 represent the piezoelectric natural frequencies. The measured piezoelectric natural frequencies were listed in Table 3 and compared with calculated values.

3.3. Discussion

It appears that the difference between the theoretical and numerical results is about 10% even though the values calculated theoretically by isotropic analysis and those calculated by FEM show better agreement. The error in the theoretical result seems to be caused by the approximation in the derivation of anisotropic analysis.

As seen in Table 3, the theoretical values calculated through the anisotropic analysis agree with the measured values within 10% error. Another reason of the frequency error seems to be the assumption of

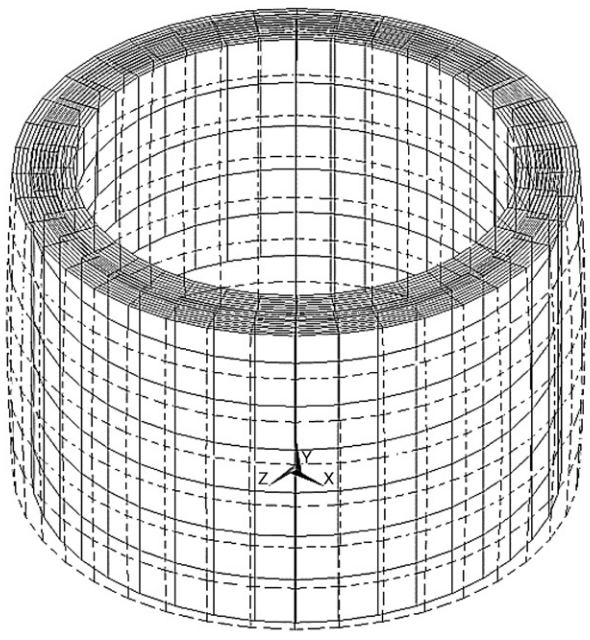

Fig. 3. Fundamental mode of the radial vibration obtained for transducer A by FEM.

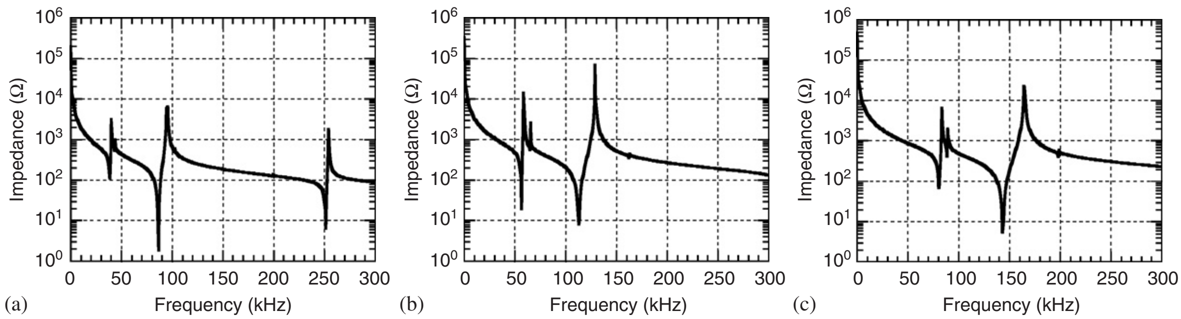

Fig. 4. Impedance curves of the piezoelectric transducers, as measured as a function of frequency; (a) transducer A, (b) transducer B, and (c) transducer C.

one-dimensional theory. The theory did not consider the mode along the thickness, while the piezoelectric cylinder used for the experiment is not a thin ring.

Within the range of the error, the analysis described in Section 2 appeared to explain the vibration characteristics of piezoelectric cylindrical transducers. Particularly it can be useful in the design stage in determining the size of a transducer for a particular frequency.

4. Conclusion

The vibration characteristics of piezoelectric cylindrical transducers were studied by deriving a characteristic equation for resonance of radial vibrations. The piezoelectric natural frequencies of the transducers were calculated from the theoretical formulae and then compared with numerical and experimental values. This comparison verifies that the theoretical results of the analysis taking into account the piezoelectric anisotropy agree well with the experimental results within 10% error. The error was caused by the elimination of a term during a derivation to obtain solvable equations. Comparison shows that isotropic analysis is also a reasonable approach to estimate the fundamental natural frequency of piezoelectric transducers.

Acknowledgement

This work was supported by the Soongsil University Research Fund.

References

[1] I.J. Busch-Vishniac, *Electromechanical Sensors and Actuators*, Springer, New York, 1999 (Chapter 5).
[2] T. Ikeda, *Fundamentals of Piezoelectricity*, Oxford University Press, Oxford, 1996.
[3] J.O. Kim, O.S. Kwon, Vibration characteristics of piezoelectric torsional transducers, *Journal of Sound and Vibration* 264 (2003) 453–473.
[4] P. Lu, K.H. Lee, W.Z. Lin, F. Shen, S.P. Lim, An approximate frequency formula for piezoelectric circular cylindrical shells, *Journal of Sound and Vibration* 242 (2001) 309–320.
[5] D.-Y. Shin, P. Grassia, B. Derby, Oscillatory limited compressible fluid flow induced by the radial motion of a thick-walled piezoelectric tube, *Journal of the Acoustical Society of America* 114 (2003) 1314–1321.
[6] J.O. Kim, K.K. Hwang, H.H. Bau, A study for the measurement of a fluid density in a pipe using elastic waves, *The Journal of the Korean Society for Nondestructive Testing* 23 (2003) 583–593.
[7] R.A. Langevin, The electro-acoustic sensitivity of cylindrical ceramic tubes, *Journal of the Acoustical Society of America* 26 (1954) 421–427.
[8] P. Heyliger, A note on the static behavior of simply-supported laminated piezoelectric cylinders, *International Journal of Solids and Structures* 34 (1997) 3781–3794.
[9] D.D. Ebenezer, P. Abraham, Eigenfunction analysis of radially polarized piezoelectric cylindrical shells of finite length, *Journal of the Acoustical Society of America* 102 (1997) 1549–1558.
[10] J.F. Haskins, J.L. Walsh, Vibrations of ferroelectric cylindrical shells with transverse isotropy. I. Radially polarized case, *Journal of the Acoustical Society of America* 29 (1957) 729–734.

[11] V.N. Lazutkin, Y.V. Tsyganov, Axisymmetric modes and electrical impedance of radially polarized piezoelectric ceramic rings, *Soviet Physics—Acoustics* 17 (1972) 330–334.

[12] N.T. Adelman, Y. Stavsky, E. Segal, Axisymmetric vibrations of radially polarized piezoelectric ceramic cylinders, *Journal of Sound and Vibration* 38 (1975) 245–254.

[13] J.O. Kim, K.K. Hwang, H.G. Jeong, Radial vibration characteristics of piezoelectric cylindrical transducers, *Journal of Sound and Vibration* 276 (2004) 1135–1144.

[14] S.G. Lekhnitskii, *Theory of Elasticity of an Anisotropic Elastic Body*, Holden-Day, San Francisco, 1963.

[15] J.D. Achenbach, *Wave Propagation in Elastic Solids*, North Holland, Amsterdam, 1975 (Chapter 2).

[16] D.K. Miu, *Mechatronics*, Springer, New York, 1993 (Chapter 6).

[17] S. Wolfram, *The Mathematica Book*, Wolfram Media, Champaign, 1999.

[18] D.A. Berlincourt, C. Cmolik, J. Jaffe, Piezoelectric properties of polycrystalline lead titanate zirconate compositions, *Proceedings of the IRE* (1960) 220–229.